



## Research Article

## Tracking control for Pneumatic muscle actuators with unknown dynamics and output constraints

Xingchen Li<sup>a,b</sup>, Xifeng Gao<sup>c,d,\*</sup><sup>a</sup> School of Mechanical Engineering, Guangdong Ocean University, Zhanjiang 524088, China<sup>b</sup> Guangdong Engineering Technology Research Center of Ocean Equipment and Manufacturing, Zhanjiang 524088, China<sup>c</sup> Center of Ultra-Precision Optoelectronic Instrumentation Engineering, Harbin Institute of Technology, Harbin 150001, China<sup>d</sup> Key Lab of Ultra-Precision Intelligent Instrumentation, Ministry of Industry Information Technology, Harbin 150080, China

## ARTICLE INFO

## Article history:

Received 14 January 2025

Revised 26 May 2025

Accepted 24 June 2025

Available online 22 July 2025

## Keywords:

Pneumatic muscle actuators (PMAs)

Unknown dynamics

Tracking control

Assigned accuracy

Output constraints

## ABSTRACT

Among the various soft actuators explored for robotic applications, the pneumatic muscle actuators (PMAs) stand out because of many advantages, such as compliant structures, high power-to-weight/volume ratios, and lightweight materials. Despite these advantages, their inherent nonlinearities and time-varying dynamics pose significant challenges for tracking control. To tackle this challenge, we present a robust control method that is structurally simple and computationally inexpensive. Such a method is comprised of an error transformation scheme, which is deeply explored to withstand model uncertainties to accomplish the output tracking with assigned accuracy, and a tuning function for relaxing requirements on the initial conditions. Experimental results of the PMA are presented to validate the concepts.

© 2025 The Author(s). Published by Elsevier B.V. on behalf of Shandong University. This is an open access article under the CC BY license (<http://creativecommons.org/licenses/by/4.0/>).

## 1. Introduction

Despite initially being aimed at purely industrial or scientific purposes, robots are now on the verge of democratizing in many different sectors of society, such as home automation [1], medicine [2,3], education [4], and even entertainment [5]. Gears and motors constitute the core foundation of many robotic platforms currently in use. However, with the rapidly growing interest in soft robots inspired by bionic principles, the exploration of efficient soft actuators has become a key research focus for laboratories worldwide [6–12]. Pneumatic muscle actuators (PMAs) are among the most common soft actuators, characterized by compliant structures, lightweight materials, and high power-to-weight and power-to-volume ratios, making them highly sought after in the soft robotics community [11,12].

Even in a relatively short period, PMAs have made significant progress, including structure designing, advanced manufacturing, and assembly strategies [11]. There is no doubt that manufacturing and integration techniques will continue to evolve, accelerating the design and application of PMAs at an unprecedented pace. As an example of the PMAs, Festo Fluidic Muscles (FFMs) have ventured beyond the laboratory and been commercialized, targeting engineering practice. However, due to strong nonlinearities and time-varying characteristics, most demonstrations using

PMAs have faced the tracking control problem that must be dealt with head-on to make continued progress.

With regard to the current control schemes of PMAs, two categories can be generally found: (1) ones for which the model information is required; and (2) ones for which model information is avoided. The former, referred to as model-based control methods, typically employs either a theoretical model, which is derived from the PMA's geometric structure and material properties [13], or a phenomenological model, which is empirically based on the relationship between input and output [14], to design control strategies [14–16]. Typically, with the help of inherent robustness, sliding mode control (SMC) techniques are introduced to compensate for the uncertainties [17–19]. Qin et al. [20] employed the Bouc–Wen model to compensate for nonlinear hysteresis, utilizing an unscented Kalman filter (UKF) to estimate the state and modeling error, thereby enhancing the performance of the nominal controller, while Liu et al. [21] focused on developing an adaptive control system by integrating a PI controller within the Bouc–Wen hysteresis model. In addition to complex mathematical models, some learning-based models derived from experimental data can also serve as control strategies, such as iterative learning [22] and spiking neuron networks (SNNs) [23]. For model-based control methods, performance heavily depends on the accuracy of the employed model. Moreover, the complexity of the model directly influences the complexity of the corresponding controller. Consequently, discrepancies between the expected and actual behavior often arise due to various uncertainties, such as friction and time-varying characteristics.

\* Corresponding author.

E-mail address: [xifenggao@hit.edu.cn](mailto:xifenggao@hit.edu.cn) (X. Gao).

The latter, herein called model-free control methods, is much more widely used due to obviating the need for model information. The PID-type control methods are undoubtedly one of the most used schemes to control the PMAs [24–26]. Furthermore, the combination of the controllers and auxiliary approximation structures (e.g., neural networks [27,28] and fuzzy logic [29,30]) is beneficial because of the excellent approximation capability. Despite the application of the aforementioned methods in the tracking control of PMAs, several limitations persist. As noted in [31], an acceptable tracking performance for the PID-type control methods [24–26] stems from a time-consuming “trial and error” process. Additionally, once the controllers are introduced into approximation structures [27–30], the well-recognized issue being addressed remains the same for these: an extra pre-training procedure and computational burden. Note that PMAs are made of highly nonlinear material, whose characteristics vary with the temperature in the case of working in long-hour scenarios. However, the efficiency of methods is limited to a specific region due to the weak robustness against high nonlinearities and time-varying characteristics. To address this issue, adaptive techniques have been incorporated into controllers to enable automatic gain adjustment [32–35]. However, this method inevitably increases the structural complexity of the controller. To address uncertainties, reinforcement learning-based controllers [36,37] are directly employed to learn control strategies; however, they require a large amount of data and additional training time. Moreover, the data-driven model-free adaptive controller (MFAC) [38,39] utilizes historical data to estimate control parameters online and dynamically adjust the control strategy in real time, thereby addressing the modeling challenges and inherent uncertainties in PMAs without requiring model training.

Beyond eliminating the reliance on model information in tracking control of PMAs, engineering practice places great emphasis on user-defined transient and steady-state performance across control methods. The same idea is behind the promising methods in [40–46] for closed-loop systems. However, uniformly ultimate boundedness (UUB) is guaranteed. Furthermore, to compensate system uncertainties, these methods also involve adaptive techniques or approximation structures [40–46]. Moreover, the operation of having to reselect some controller parameters is required when the task is reassigned, which is inconvenient for practical applications. In addition, all real-world systems are faced with output constraints coming from specifications of operation and considerations of safety. From a practical standpoint, the controller should be structurally simple, computationally efficient, and user-friendly, while minimizing the reliance on specialized hardware. These considerations are essential in the continued development of the control method.

Motivated by the previous discussions making great strides in the challenges of tracking control for PMAs, this paper focuses on the tracking control problem for PMAs subject to unknown dynamics, output constraints, and time-varying characteristics. A robust control method without involving approximation structures or adaptive techniques is provided for solving the above problem in practice. The basic idea behind the presented controller is structurally simple, computationally inexpensive, and easy to be used. No hard calculation of analytic derivatives demanded in backstepping design is conducted from a theoretical perspective. By exploring the potential robustness of an error transformation technique in-depth, the presented method can accomplish the tracking control of the PMA, avoiding a high cost in building or maintaining complex models of PMAs.

This paper is organized as follows. An overview of the most commonly utilized models for PMAs is provided in Section 2.1. Section 2.2 gives the description of output constraints. This is followed by Section 2.3 in which we propose a task description

required to be accomplished in the tracking control. Next, in Section 3, we design the controller to address the task description in Section 2.3. Then, Section 4 gives the stability analysis. Section 5 experimentally demonstrates the performance of the presented control method using a PMA system. In Section 6, we conclude this paper and offer suggestions for further work.

## 2. System description and problem formulation

### 2.1. System description

The most commonly utilized model for describing PMAs is the three-element model, as described in Fig. 1, which is composed of the spring element  $K(P)$ , damping element  $B(P)$ , and contractile element  $F(P)$ . According to [17,28,35], the overall system is obtained as

$$\begin{cases} m\ddot{x}_s(t) + B(P)\dot{x}_s(t) + K(P)x_s(t) = F(P) - mg \\ B(P) = B_0 - B_1P(t) \\ K(P) = K_0 - K_1P(t) \\ F(P) = F_0 + F_1P(t) \end{cases} \quad (1)$$

where  $x_s(t)$  denotes the amount of PMA contraction.  $m$ ,  $P(t)$ , and  $g$  are the mass of load, the air pressure of the PMA, and the gravitational acceleration, respectively.  $B_0$ ,  $B_1$ ,  $K_0$ ,  $K_1$ ,  $F_0$ , and  $F_1$  correspond to the polynomial coefficients. In practice, the mass of load  $m$  is changed according to different working scenarios, which can be formulated as follows:

$$m = m_0 + \Delta m \quad (2)$$

where  $m_0$  stands for the nominal mass, and  $\Delta m$  is the change of mass  $m$ . Precisely, the internal air pressure of PMA can be expressed as

$$P(t) = p_0(t) + \Delta p(t) \quad (3)$$

where  $p_0(t)$  represents the initial air pressure inside the PMA, and  $\Delta p(t)$  denotes the variation of air pressure of the PMA. Because of PMAs possessing two equilibrium points at  $x_s(t)$  and  $x_0$ , we have  $\ddot{x}_s(t) = \ddot{x}_0 = 0$  and  $\dot{x}_s(t) = \dot{x}_0 = 0$ . At initial time, we preset the initial pressure  $p_0(t)$  to fix the PMA displacement  $x_0$ . According to (1) and (2), one has

$$F(p_0) - K(p_0)x_0 = (m_0 + \Delta m)g \quad (4)$$

According to (3) and the above analysis, we have

$$u(t) = \Delta p(t) = P(t) - p_0(t) \quad (5)$$

$$x(t) = x_s(t) - x_0 \quad (6)$$

Combining (1), (2), (4), (5), and (6), the model of PMAs can be rewritten as

$$\ddot{x}(t) = H(t)u(t) - D(t)\dot{x}(t) - G(t)x(t) \quad (7)$$

where

$$\begin{cases} D(t) = (B_0 - B_1p_0(t)) / (m_0 + \Delta m) \\ G(t) = (K_0 - K_1p_0(t)) / (m_0 + \Delta m) \\ H(t) = l\dot{x}(t) + bx(t) + f \end{cases}$$

with  $l = B_1/(m_0 + \Delta m)$ ,  $b = K_1/(m_0 + \Delta m)$ , and  $f = (F_1 + K_1x_0)/(m_0 + \Delta m)$ .

**Remark 1.** As pointed out at [14–16], it is worth noting that the higher-order terms in  $B(P)$ ,  $K(P)$ , and  $F(P)$  provide higher approximation accuracy, but increase complexity in the model. Meanwhile, the polynomial coefficients (i.e.,  $B_0$ ,  $B_1$ ,  $K_0$ ,  $K_1$ ,  $F_0$ , and  $F_1$ ) are changed when the air pressure of the PMA  $P(t)$  lies in different values. However, from a practical point of view, the simple model (i.e., the Reynolds model) is usually considered. Further details regarding this description can be found in [17,28,35].

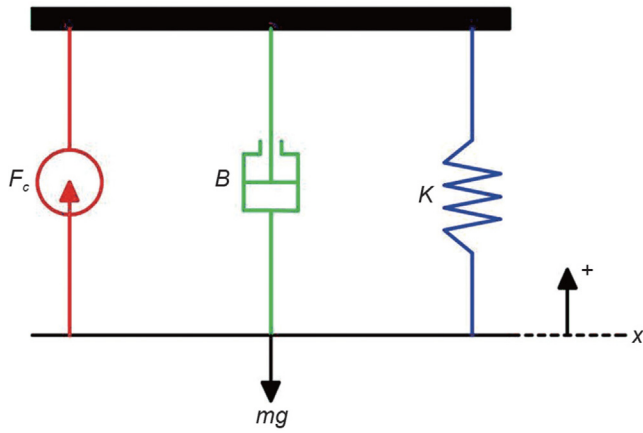


Fig. 1. Three-element model of PMA systems.

**Remark 2.** Over the last decade, there has been an explosion of work in the tracking control of PMAs. In particular, the polynomial coefficients (i.e.,  $B_0, B_1, K_0, K_1, F_0,$  and  $F_1$ ) are required to be known in [14–16]. Recent surveys in [17,28,32,35] still highlight the need for estimating polynomial coefficients when dealing with the tracking control of PMAs. Nevertheless, in this paper, the polynomial coefficients (i.e.,  $B_0, B_1, K_0, K_1, F_0,$  and  $F_1$ ) are unknown.

After the model is introduced, the problem formulation needs to be presented in the subsection. This paper forces on the tracking control problem. The control objective of (7) is to perform output tracking, i.e., the position  $x(t)$  is demanded to track the reference trajectory  $x_r(t)$ . The tracking error is expressed as

$$e(t) = x(t) - x_r(t) \quad (8)$$

### 2.2. Output constraints

In practice, many systems have physical constraints for the safe operation or preventing equipment damage. Since the maximum displacement of PMAs is 30% of the initial length [11,13], a sort of position constraint for (7) is considered as

$$\underline{k}(t) < x(t) < \bar{k}(t), \quad \forall t \geq 0 \quad (9)$$

where  $\underline{k}(t)$  denotes the lower constraint boundary, and  $\bar{k}(t)$  represents the upper constraint boundary. In the PMA systems, a precondition on (9) is taken into consideration, i.e.,

$$\underline{k}(0) \leq x(0) < \bar{k}(0) \quad (10)$$

By using (8), (9) is converted into

$$\underline{k}(t) - x_r(t) < e(t) < \bar{k}(t) - x_r(t), \quad \forall t \geq 0 \quad (11)$$

An assumption borrowed from the existing work [47], is exploited for the subsequent development below.

**Assumption 1.** There exist two positive constants  $\underline{q}$  and  $\bar{q}$ , which satisfies the following inequality, i.e.,

$$\underline{q} < \bar{k}(t) - \underline{k}(t) < \bar{q}, \quad t \geq 0 \quad (12)$$

### 2.3. Problem formulation

**Problem 1.** Consider PMAs (7) with unknown nonlinear dynamics. The objective is to design a robust control method such that

the system (7) output tracks the reference trajectory with the assigned accuracy  $w_1$ , i.e.,

$$\lim_{t \rightarrow \infty} |e(t)| < w_1 \quad (13)$$

The assigned tracking accuracy  $w_1$  is a positive design parameter with  $w_1 > 0$ . All closed-loop signals remain bounded, and the specified output constraint is strictly respected throughout the operation.

Consider Assumption 1 and the assigned tracking accuracy  $w_1$  under output constraint (11). We have the following inequality

$$\underline{k}(t) - x_r(t) < \underline{w}_1 < \bar{w}_1 < \bar{k}(t) - x_r(t) \quad (14)$$

Here, for the subsequent development, one assumption that is the wide-scale adoption in the literature [32,35,40–46] and reasonable in practice [13–16], is introduced and motivates the accomplishment of stability analysis in the following work.

**Assumption 2.** The reference trajectory  $x_r(t)$  keeps in the set  $(\underline{k}(t), \bar{k}(t))$ , and its first-order derivative  $\dot{x}_r(t)$  maintain bounded.

### 3. Controller design

To achieve the above problem, we design a robust controller. The first step toward the presented controller is related to the tuning function  $\alpha(t)$  with the following form [48]

$$\alpha(t) = \begin{cases} -\frac{1}{2} \cos\left(\pi \frac{t}{t_u}\right) + \frac{1}{2}, & t < t_u \\ 1, & t \geq t_u \end{cases} \quad (15)$$

where  $t_u > 0$  is a design parameter. Through making use of (8) and (15), the modified position error is given by

$$\lambda_1(t) = \alpha(t)e(t) \quad (16)$$

Subsequently, the virtual control law is presented as

$$\theta(t) = -a\chi(t) \quad (17)$$

with

$$\chi(t) = \tan\left(\frac{\pi\lambda_1(t)}{2w_1}\right) \quad (18)$$

where  $a > 0$  is a design parameter. Using (15), the velocity error can be written as follows:

$$\lambda_2(t) = \alpha(t)\dot{x}(t) - \theta(t) \quad (19)$$

Finally, let us define the control law as follows:

$$u(t) = -c\beta(t)\delta(t) \quad (20)$$

with

$$\beta(t) = \frac{1}{w_2 \cos^2\left(\frac{\pi\lambda_2(t)}{2w_2}\right)} \quad (21)$$

and

$$\delta(t) = \tan\left(\frac{\pi\lambda_2(t)}{2w_2}\right) \quad (22)$$

where  $c > 0$  and  $w_2 > 0$  are design parameters.

It is worth noting that the tuning function  $\alpha$  is designed to regulate both the position tracking error and velocity. Without this function, the initial position error and velocity of PMAs are strictly constrained within their assigned bounds. However, its incorporation allows the initial position error to exceed the predefined limit, thereby effectively relaxing the constraints on initial conditions.

**Remark 3.** Significant progress has recently been achieved in the position control of PMAs, particularly through the development of controllers that utilize approximation structures [27–30,42,46] or adaptive techniques [32,33,35,40–45] to estimate unknown nonlinear terms or compensate for nonlinearities. In this paper, these structures or techniques are evaded in the control design, regardless of unknown nonlinear dynamics. The presented method is distinguished by its structural and computational simplicity, eliminating the need for complex analytic derivative calculations typically required in backstepping designs [17,18,32,35] is conducted. This streamlined method not only reduces computational burden but also enhances practical usability.

#### 4. Stability analysis

This section proposes the main result. Here, the stability analysis begins with the following lemmas. Specifically, Lemmas 1 and 2 are borrowed from the previous work, and further details regarding the proof process can be found in [43]. Lemma 3 and its proof are given below. Subsequently, we propose the main result in Theorem 1 using the following lemmas and Assumption 1 and 2. Before moving on to the main result, three lemmas are given.

**Lemma 1.** For any continuously differentiable function  $f(t)$  with an initial value of  $f(0)$ , we have the following properties.

- (1) If  $\alpha(t)f(t)$  keeps bounded, then  $f(t)$  is bounded.
- (2) If  $f(t)$  methods infinity, then  $\alpha(t)f(t)$  methods infinity.

**Lemma 2.** For  $t \geq 0$ , if  $w_1 < e(t) < \bar{w}_1$  holds, then the tracking error cannot violate the output constraints.

**Lemma 3.** If  $\chi(t)$  and  $\dot{\lambda}_1(t)$  maintain bounded, and  $|\lambda_1(t)| < w_1$  holds, then  $\dot{\theta}(t)$  keeps bounded.

**Proof of Lemma 3.** First of all, differentiating (18) yields

$$\dot{\chi}(t) = \frac{\pi}{2} \frac{1}{\cos^2\left(\frac{\pi}{2} \frac{\lambda_1(t)}{w_1}\right)} \left(\frac{\dot{\lambda}_1(t)}{w_1}\right) \quad (23)$$

After that, by differentiating (17) and using (23), one has

$$\dot{\theta}(t) = -a \frac{\pi}{2} S^{-1}(t) \left(\frac{\dot{\lambda}_1(t)}{w_1}\right) \quad (24)$$

where

$$S(t) = \cos^2\left(\frac{\pi}{2} \frac{\lambda_1(t)}{w_1}\right) \quad (25)$$

With the careful inspection of (18), it should be noted that if  $\chi(t)$  maintains bounded, then  $|\lambda_1(t)| < w_1$  holds. Further on,  $S(t)$  in (25) remains bounded. As long as  $S(t)$  and  $\dot{\lambda}_1(t)$  remain bounded, the boundedness of  $\dot{\theta}(t)$  is guaranteed. Hence, Lemma 3 is proven.

Having established the preceding lemmas, we now proceed to present the main result, stated formally as the following theorem.

**Theorem 1.** Considering the above system (7) satisfying Assumptions 1 and 2. The presented control method solves Problem 1.

**Proof of Theorem 1.** A method by seeking a contradiction takes on the subsequent sequel. We establish that

$$|\lambda_i(t)| < w_i, \quad i = 1, 2, \quad t \geq 0 \quad (26)$$

By seeking a contradiction, let us assume that opportunities exist to violate the above inequality (26), such that

$$|\lambda_i(t_f)| \geq w_i, \quad i \in \{1, 2\}, \quad f \in Z^+ \quad (27)$$

where  $t_f$  represents the first time to violate (26).

On the basis of the continuity of  $e(t)$  and  $\lambda_i(t)$ ,  $i = 1, 2$ , Assumption 2, and the controller design given beforehand, it can be obtained that there surely exists the modified tracking errors  $\lambda_i(t)$  as

$$\lim_{t \rightarrow t_f^-} |\lambda_i(t)| = w_i, \quad i \in \{1, 2\} \quad (28)$$

By recalling (15)–(19), one has

$$|\lambda_i(0)| < w_i, \quad i = 1, 2 \quad (29)$$

According to (29),  $t_f > 0$  holds. Thus, we have that

$$|\lambda_i(t)| < w_i, \quad i = 1, 2, \quad t < t_f \quad (30)$$

The analysis is presented afterward. In the following, the time argument is dropped from the above-defined variables for presentation compactness.

*Step 1:* Firstly, differentiating (16) via utilizing (8) yields

$$\dot{\lambda}_1 = \dot{\alpha}(x - x_r) + \alpha\dot{x} - \alpha\dot{x}_r \quad (31)$$

Injecting (17) and (19) into (31) gives

$$\dot{\lambda}_1 = \dot{\alpha}(x - x_r) - \alpha\dot{x}_r + \lambda_2 - a\chi \quad (32)$$

Let us define the Lyapunov function as follows:

$$V_1 = \frac{1}{\pi} \chi^2 \quad (33)$$

Differentiating (33) gets the following form

$$\dot{V}_1 = \frac{2}{\pi} \chi \dot{\chi} \quad (34)$$

Substituting (23) into (34) and using (32), one further has

$$\dot{V}_1 = \frac{1}{w_1} \chi \frac{1}{\cos^2\left(\frac{\pi}{2} \frac{\lambda_1}{w_1}\right)} (I_1 - a\chi) \quad (35)$$

where

$$I_1 = \dot{\alpha}(x - x_r) - \alpha\dot{x}_r + \lambda_2$$

Subsequently, the boundedness of  $I_1$  is built upon the discussions below. As mentioned previously, a  $t_f$  exists such that for  $t < t_f$ , we can obtain that (1) under Assumption 2, one has that  $\dot{x}_r$  is bounded; (2) recalling (15), it holds that  $\alpha\dot{x}_r$  and  $\dot{\alpha}$  are bounded; (3) based on (16), (30), and Lemma 1.1, one further gets that the boundedness of  $(x - x_r)$  and  $\lambda_2$  is guaranteed; and (4) according to the boundedness of  $\dot{\alpha}$  and  $(x - x_r)$ ,  $\dot{\alpha}(x - x_r)$  keeps bounded. In light of the above discussions, it can be seen that  $I_1$  keeps bounded. Thereby, there exists an inequality with the following form

$$|I_1| < \bar{I}_1, \quad t < t_f \quad (36)$$

where  $\bar{I}_1 > 0$  is a constant. Substituting (36) into (35) yields

$$\dot{V}_1 \leq \frac{1}{w_1} \frac{1}{\cos^2\left(\frac{\pi}{2} \frac{\lambda_1}{w_1}\right)} |\chi| (\bar{I}_1 - a|\chi|) \quad (37)$$

Finally, if we want to have  $\dot{V}_1 < 0$ , the underlying inequality holds

$$|\chi| > \frac{\bar{I}_1}{a}, \quad t < t_f \quad (38)$$

To this end, according to (15), it is clear that  $\alpha(0) = 0$ . Further on, from (16), one has that  $\lambda_1(0) = 0$ . As a result, by (18), we can get that  $\chi(0) = 0$ . With the aid of the analysis given above and (33), we have

$$|\chi| \leq \frac{\bar{I}_1}{a}, \quad t < t_f \quad (39)$$

Step 2: Firstly, by differentiating (22) and using (21), one has

$$\dot{\delta} = \frac{\pi}{2}\beta\dot{\lambda}_2 \quad (40)$$

Differentiating (19) leads to

$$\dot{\lambda}_2 = \dot{\alpha}\dot{x} + \alpha\ddot{x} - \dot{\theta} \quad (41)$$

Next, substitute (7), (20), and (41) into (40), which yields

$$\dot{\delta} = \frac{\pi}{2}\beta(I_2 - Hc\alpha\beta\delta) \quad (42)$$

where

$$I_2 = \dot{\alpha}\dot{x} - \dot{\theta} - \alpha(D\dot{x} + Gx) \quad (43)$$

The Lyapunov function is defined as

$$V_2 = \frac{1}{\pi}\delta^2 \quad (44)$$

Differentiating (44) via applying (42) yields

$$\dot{V}_2 = \beta\delta(I_2 - Hc\alpha\beta\delta) \quad (45)$$

Then, we are ready to establish the boundedness of  $I_2$  in ((43)) over  $[0, t_f]$ . In light of (15), (17), ((18)), (19), (30), and Lemma 1.1, it holds that  $\dot{\alpha}$  and  $\dot{x}$  are bounded, and thus  $\dot{\alpha}\dot{x}$  remains bounded. Recalling (17), (18), (30), and Lemma 3, the boundedness of  $\dot{\theta}$  is ensured. Based on (15), (16), (30), Lemma 1.1, and Assumption 2, one further gets that the boundedness of  $x$  is guaranteed. Since we face a physical system, the air pressure inside the PMA  $p_0$ , the nominal mass  $m_0$ , and the uncertain part  $\Delta m$  remain bounded. According to [14–16,32,35], the polynomial coefficients (i.e.,  $B_0$ ,  $B_1$ ,  $K_0$ ,  $K_1$ ,  $F_0$ , and  $F_1$ ) are bounded. Based on the above-mentioned points, it is found that  $I_2$  which is the sum of several bounded functions, remains bounded. As such, (43) can be expressed by using an inequality in the form

$$|I_2| < \bar{I}_2, \quad t < t_f \quad (46)$$

where  $\bar{I}_2 > 0$  is a constant. Based on [14–16,32,35], there exist some unknown constants  $\underline{H}$  and  $\bar{H}$  such that

$$0 < \underline{H} \leq |H(t)| \leq \bar{H} < \infty \quad (47)$$

According to (45), (46), and (47), we rewrite (45) explicitly as

$$\dot{V}_2 \leq |\beta\delta|(\bar{I}_2 - \underline{H}c\alpha|\beta\delta|) \quad (48)$$

Eventually, (48) shows that  $\dot{V}_2 < 0$ , which ensures

$$\alpha|\beta\delta| > \frac{\bar{I}_2}{\underline{H}c}, \quad t < t_f \quad (49)$$

Recalling (28) and Lemma 1.2, we have

$$\lim_{t \rightarrow t_f^-} \alpha|\beta\delta| = +\infty \quad (50)$$

According to (44), the following result is obtained that

$$\alpha|\beta\delta| < \frac{\bar{I}_2}{\underline{H}c}, \quad t \in [t_r, t_f) \quad (51)$$

From the above discussions (see Steps 1 and 2), it can be seen  $\lambda_1$  and  $\lambda_2$  are impossible to approach  $w_1$  and  $w_2$  as  $t < t_f$ , which means that the obtained results in (39) and (51) contradict the deduction below (27). Consequently, the supposition is invalid, and the result presented in (26) is true.

Step 3: After the discussions (see Steps 1 and 2) mentioned above, our task in this step is to discuss the boundedness of all closed-loop signals. The following description plays an important role, as below. According to the analysis results in Steps 1 and 2, we have that (26) holds for all  $t \geq 0$ . These results indicate that the computed results in (18), (21), and (22) keep bounded.

Under (19) and (26), the velocity is bounded. Further on,  $\theta$  in (17) and  $u$  in (20) are bounded. As a consequence, all closed-loop signals remain bounded. According to Lemma 2, we have that the specified output constraint is never transgressed. This completes the proof.

## 5. Experimental investigation

The above section provides stability analysis from a theoretical perspective. In order to validate the effectiveness of the control method described in Section 3, the experiments are conducted with the PMA system, and the results are presented in this section.

### 5.1. Experimental setup

In this paper, we construct a hardware platform for the PMA to evaluate the performance of our control method. This platform consists of two power supplies, an air compressor, an air filter regulator, a magnetic indicator stand (7010S-10, Mitutoyo Corp., Kawasaki, Japan), two electro-pneumatic regulators (ITV2050-312L, SMC Corp., Tokyo, Japan), a 64-bit Windows-7-based host computer with an Intel Core i7 processor @ 3.40 GHz and 16-GB RAM, a PCI data acquisition card (NI PCI-6221, National Instruments Corp., Texas, USA), a PMA (MAS-10-100N-AA-MC-O-ER-EG, Festo AG & Co. KG, Esslingen, Germany) with a length of 10 cm, a laser displacement sensor (OADM 20I2441/S14C, Baumer Electric AG, Frauenfeld, Switzerland), a mass airflow sensor (AWM5104, Honeywell Inc., NJ, USA), and a pneumatic cylinder(SC32X250, AirTAC International Group, Taiwan, China). The picture of the hardware platform is given in Fig. 2. The schematic diagram of the PMA actuated system is shown as Fig. 3. Specifically, the electro-pneumatic regular first receives the control input signal to drive the PMA movement. Then, the laser displacement sensor sends the position feedback signal of the PMA to the host computer. To demonstrate the controller's ability to resist external disturbances, the right end of the PMA is connected to a pneumatic cylinder that provides a horizontal disturbance force.

### 5.2. Experimental results

Experiments were performed to demonstrate the feasibility of the presented control method using the above experimental setup (see Fig. 2). For comparison purposes, a comparative study was made with one additional control method, i.e., the model-free adaptive control (MFAC) method [49]. It is known for its simplicity and direct data-driven method, making it a suitable baseline for evaluating the performance of other model-free controllers without the complexity of auxiliary approximation structures, such as neural networks or fuzzy logic. In all experiments, the reference trajectory was intentionally designed to start away from the actuator's initial position, effectively introducing step-like conditions. This setup demonstrates that the proposed controller relaxes the requirement on the initial alignment with the reference trajectory, highlighting its robustness and adaptability to practical variations.

Case 1: In this case, we demonstrate that the presented control method can manage the position tracking with the assigned accuracy  $w_1$ . Note that the air is entered into the pneumatic cylinder from port B. Before performing the experiment, the presented control method was uploaded to the PC. After that, the PMA was requested to track the reference trajectory  $x_r = -0.5 \sin t - 2$ . Further on, controller parameters were set to  $t_u = 6$ ,  $a = 2$ ,  $c = 2$ ,



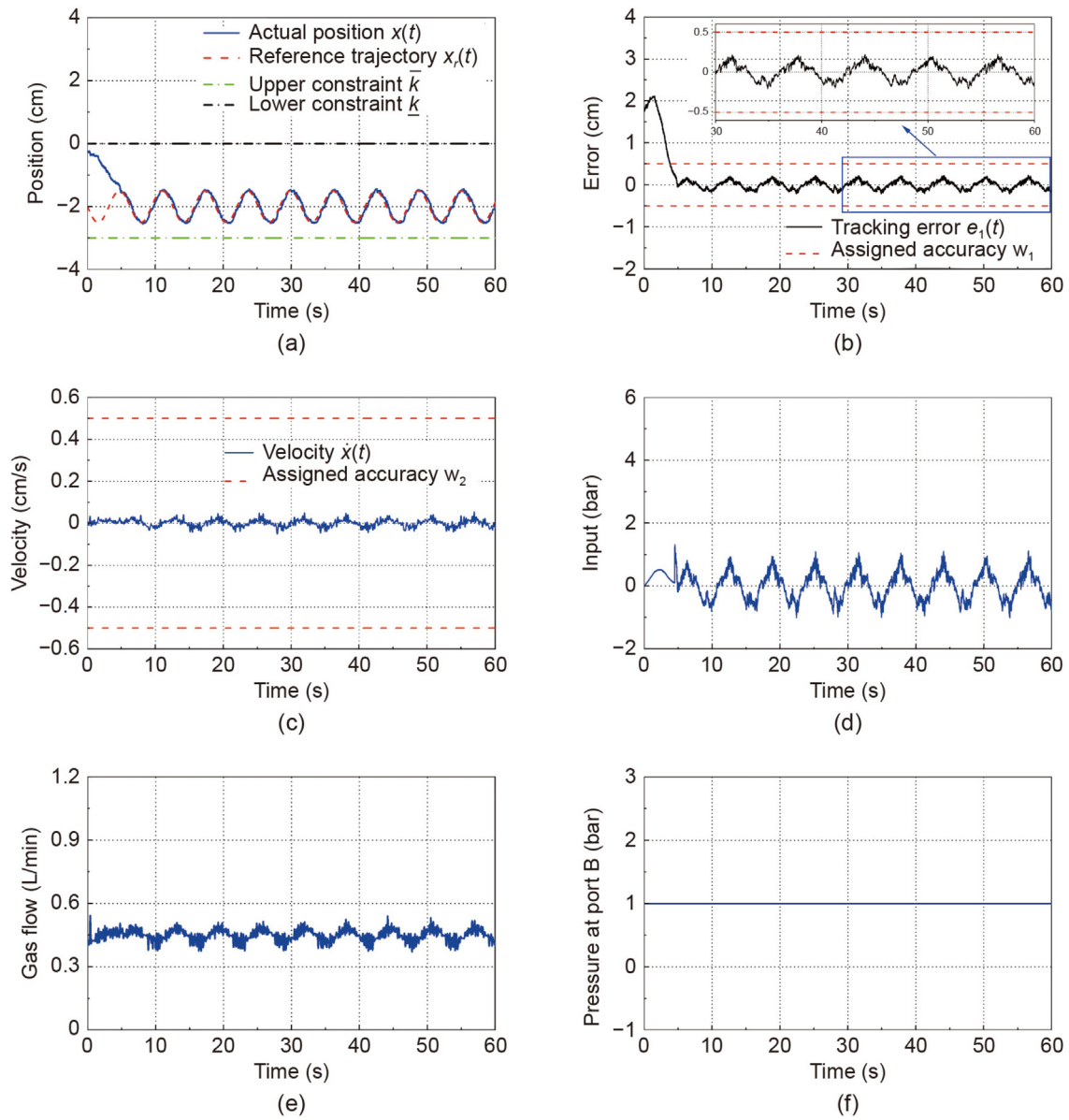


**Fig. 4.** Results utilizing the presented controller ( $t_u = 6, w_1 = 0.5$ ). (a) Measured position and the reference position ( $x(t)$  and  $x_r(t)$ ). (b) Error between the measured position and the reference position ( $e(t)$  and  $w_1$ ). (c) Velocity of the PMA ( $\dot{x}(t)$ ). (d) Change of the control input ( $u(t)$ ). (e) Airflow of the PMA. (f) Air pressure at port B.

**Table 1**  
RMSTE of different controller parameters in Cases 1 and 2.

Parameters	Periods (s)				
	10–20	20–30	30–40	40–50	50–60
$t_u = 6, w_1 = 0.5$	0.0969	0.0970	0.0972	0.0993	0.1013
$t_u = 6, w_1 = 0.3$	0.0891	0.0852	0.0866	0.0878	0.0875
$t_u = 2, w_1 = 0.3$	0.0842	0.0827	0.0835	0.0866	0.0847

system behavior. To this end, the same reference trajectory was still performed to accomplish tracking control of the PMA. Considering the same experiment conditions in Fig. 5, all controller parameters were selected as the same values except for the parameter  $t_u$ , which was set to  $t_u = 2$ . (see Fig. 6).

As illustrated in Fig. 6, the value of the parameter  $t_u$  indeed influences the system performance. The transient performance at which the position tracking error  $e(t)$  starts to converge to

the assigned accuracy, improves with decreasing the value of the parameter  $t_u$  (see Figs. 5(a), 5(b), 6(a), and 6(b)). In addition, decreasing the value of the parameter  $t_u$  adversely increases the value of the velocity  $\dot{x}(t)$  (see Figs. 5(c) and 6(c)), and the peak values of control inputs  $u(t)$  have a significant influence in the initial stage (see Figs. 5(d) and 6(d)). Since the parameters  $w_2$  and  $c$  are not changed in this case, the steady-state error has no significant influence (see Figs. 5(b) and 6(b)). We can see that from a practical point of view, the choice of the parameter  $t_u$  is based on the trade-off between the maximum output of the actuator and a user-acceptable convergence time. For example, to achieve the tracking control with a large initial value during a very short time, the actuator produces a huge output. The tracking performance of the presented controller in steady state-phase is quantified using RMSTE, and the results for this case are shown in Table 1. It is evident that the steady-state errors in both situations show no significant difference.

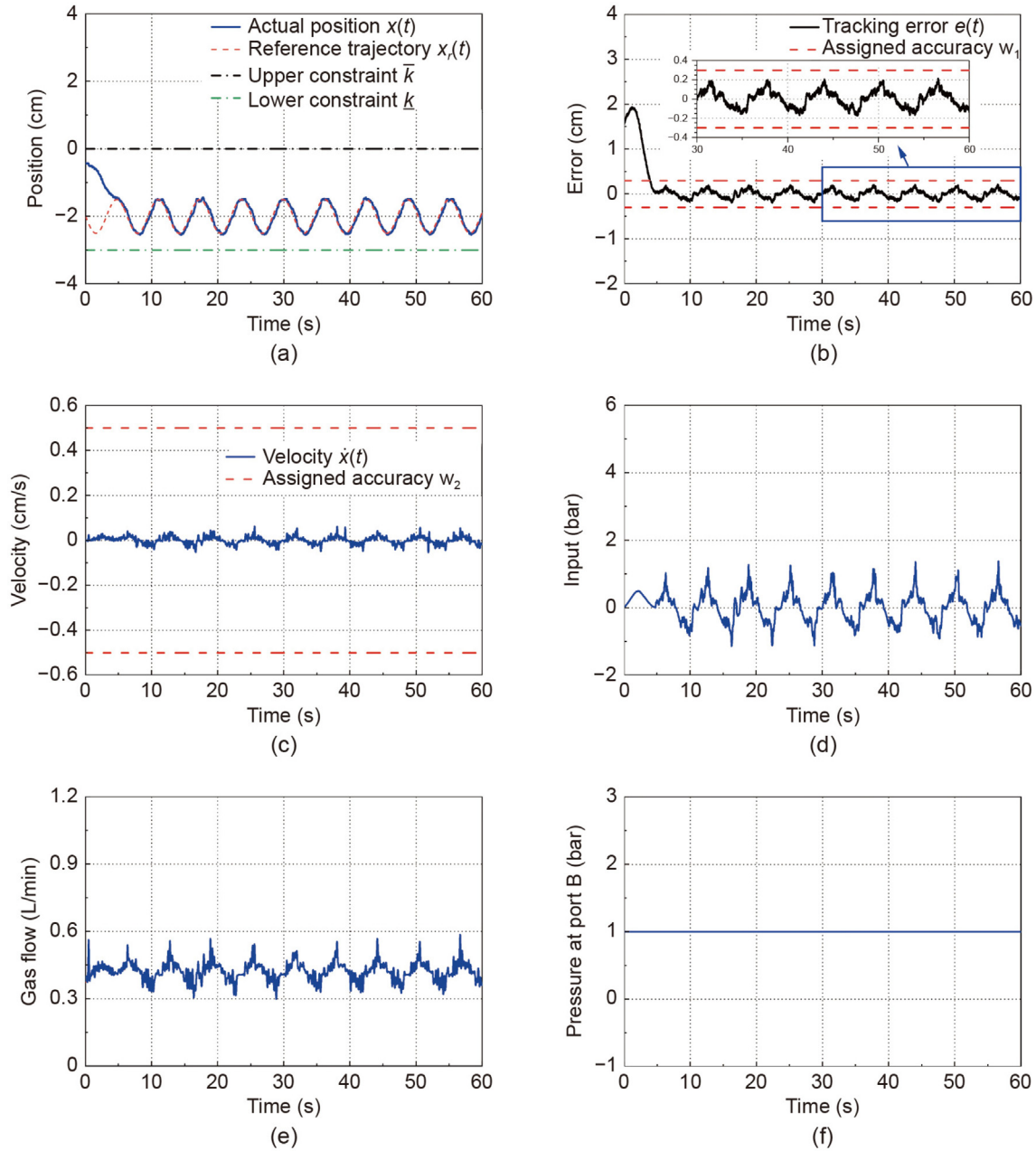


**Fig. 5.** Results utilizing the presented controller ( $t_u = 6$ ,  $w_1 = 0.3$ ). (a) Measured position and the reference position ( $x(t)$  and  $x_r(t)$ ). (b) Error between the measured position and the reference position ( $e(t)$  and  $w_1$ ). (c) Velocity of the PMA ( $\dot{x}(t)$ ). (d) Change of the control input ( $u(t)$ ). (e) Airflow of the PMA. (f) Air pressure at port B.

**Case 3:** Here, we demonstrate that the presented control method can accomplish tracking control of the PMA under unknown dynamics. Before performing the experiment, the presented control method was uploaded to the PC. After that, the PMA was requested to track the reference trajectory  $x_r = t \sin(2\pi t(1+t/55)/55 - \pi/2)/360 - 2$  with the varying amplitude and frequency. Further on, controller parameters were set to  $t_u = 2$ ,  $a = 2$ ,  $c = 2$ ,  $w_2 = 0.5$ ,  $w_1 = 0.2$ ,  $\underline{k} = 0$ , and  $\bar{k} = -3$ . In the following experiments, the air entered into the pneumatic cylinder from port A at  $t = 20$  s to provide the external disturbance. For the sake of comparison, the MFAC method is employed. Unless stated otherwise, the same trajectory and test conditions were employed. Along this line, the parameters in the MFAC method were selected as  $\eta = 0.5$ ,  $\mu = 1.9$ ,  $\rho = 31.7$ , and  $\lambda = 0.03$ . Figs. 7 and 8 illustrate the results obtained for

the experimental demonstration by running the same platform, where the presented control method and the MFAC method were considered, respectively.

More specifically, the presented control method and the MFAC method both have the ability to realize tracking control. At the initial stage (see Figs. 7(a) and 8(a)), the similar behavior has been shown by using two control methods. However, when the amplitude and frequency of the reference trajectory increase, the steady-state error gained by employing the MFAC method increases noticeably as time goes on (see Fig. 7(b) and Fig. 8(b)). RTSME is employed to quantitatively evaluate the tracking performance of the two control algorithms, as shown in Table 2. Evidently, the presented method exhibits superior steady-state performance. In addition, it can be seen that utilizing the presented control method guarantees that the steady-state error

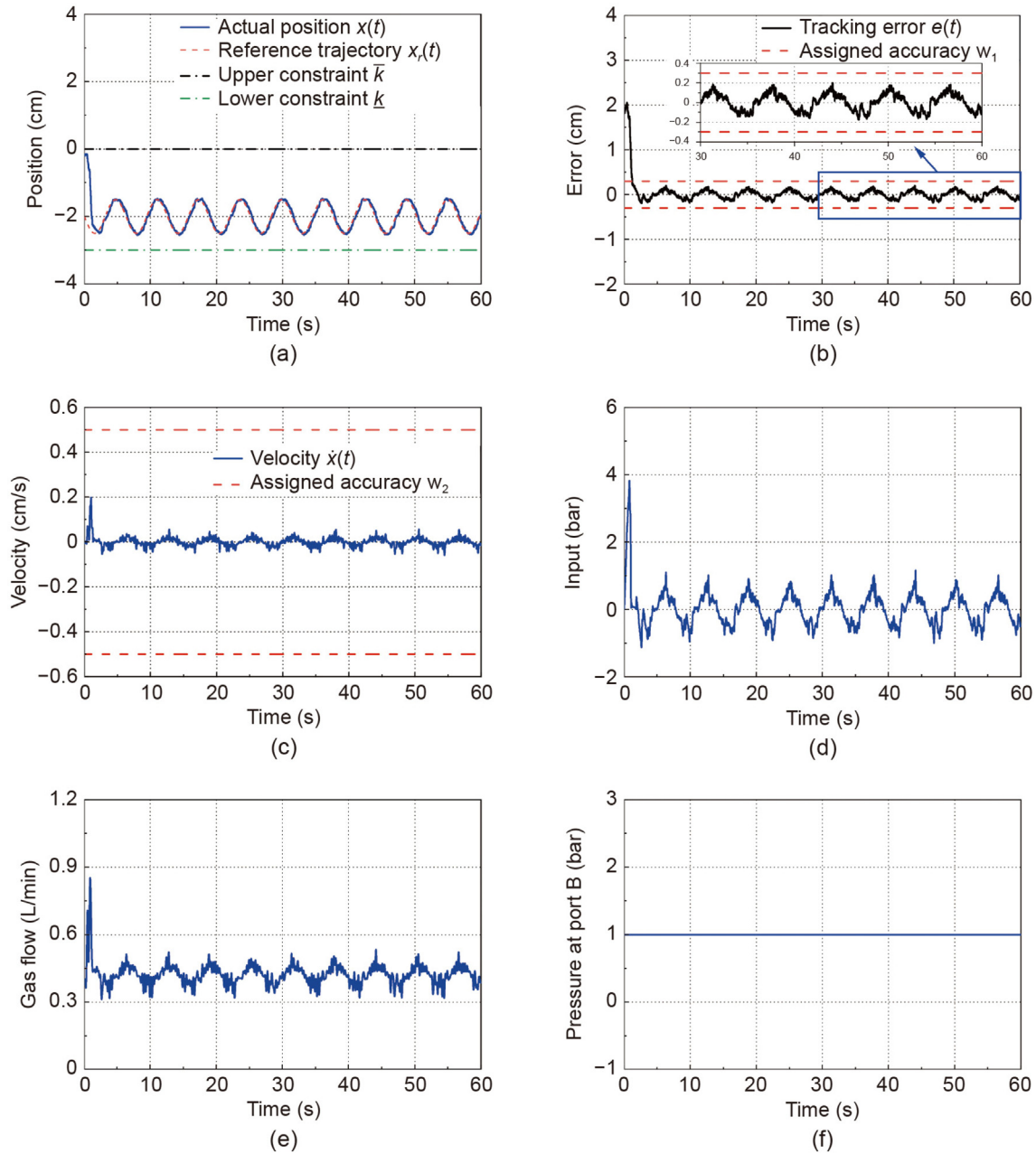


**Fig. 6.** Results utilizing the presented controller ( $t_u = 2$ ,  $w_1 = 0.3$ ). (a) Measured position and the reference position ( $x(t)$  and  $x_r(t)$ ). (b) Error between the measured position and the reference position ( $e(t)$  and  $w_1$ ). (c) Velocity of the PMA ( $\dot{x}(t)$ ). (d) Change of the control input ( $u(t)$ ). (e) Airflow of the PMA. (f) Air pressure at port B.

converges to the specified accuracy bounds ( $w_1 = 0.2$ ) within the specified time, and the steady-state error cannot escape the specified accuracy bounds as time goes on. On the contrary, The steady-state error of MFAC method exceeds 0.2 in the later stage of tracking (see Fig. 8(b)). Figs. 7(d) and 8(d) can give the reason to explain this phenomenon. The presented control method can quickly adjust the control input to finish the position tracking when the frequency and amplitude of the reference trajectory are changed. However, the MFAC method cannot achieve it in this case, which works on the measured input/output data and is based on off-line parameters. According to the results, it can be seen that the presented control method is capable of working in the position tracking of the PMA with unknown dynamics, unpredictable disturbances, and output constraints.

**Table 2**  
RMSTE of different Controllers in Case 3.

method	Periods (s)					
	5-30	30-60	60-90	90-120	120-150	150-180
Presented	0.0110	0.0144	0.0207	0.0329	0.0435	0.0590
MFAC	0.0128	0.0212	0.0404	0.0746	0.0993	0.1439

## 6. Conclusion

This paper introduces a control method for the PMAs, which is structurally simple, computationally inexpensive, and easy to be used. Built upon a tuning function and an error transformation scheme, this method is capable of implementing the position

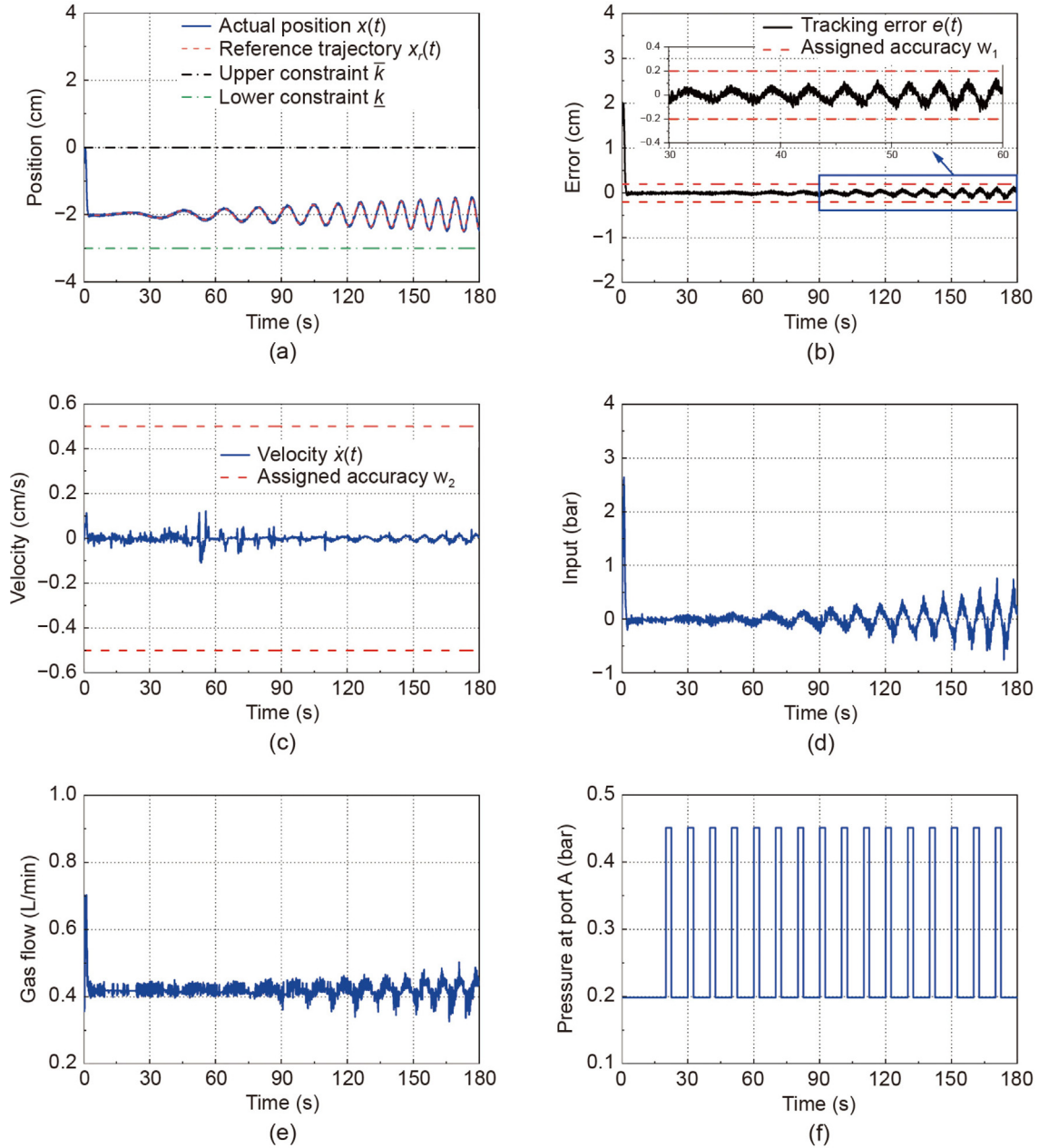


**Fig. 7.** Results employing the presented controller. (a) Measured position and the reference position ( $x(t)$  and  $x_r(t)$ ). (b) Error between the measured position and the reference position ( $e(t)$  and  $w_1$ ). (c) Velocity of the PMA ( $\dot{x}(t)$ ). (d) Change of the control input ( $u(t)$  and  $w_2$ ). (e) Airflow of the PMA. (f) Air pressure at port A.

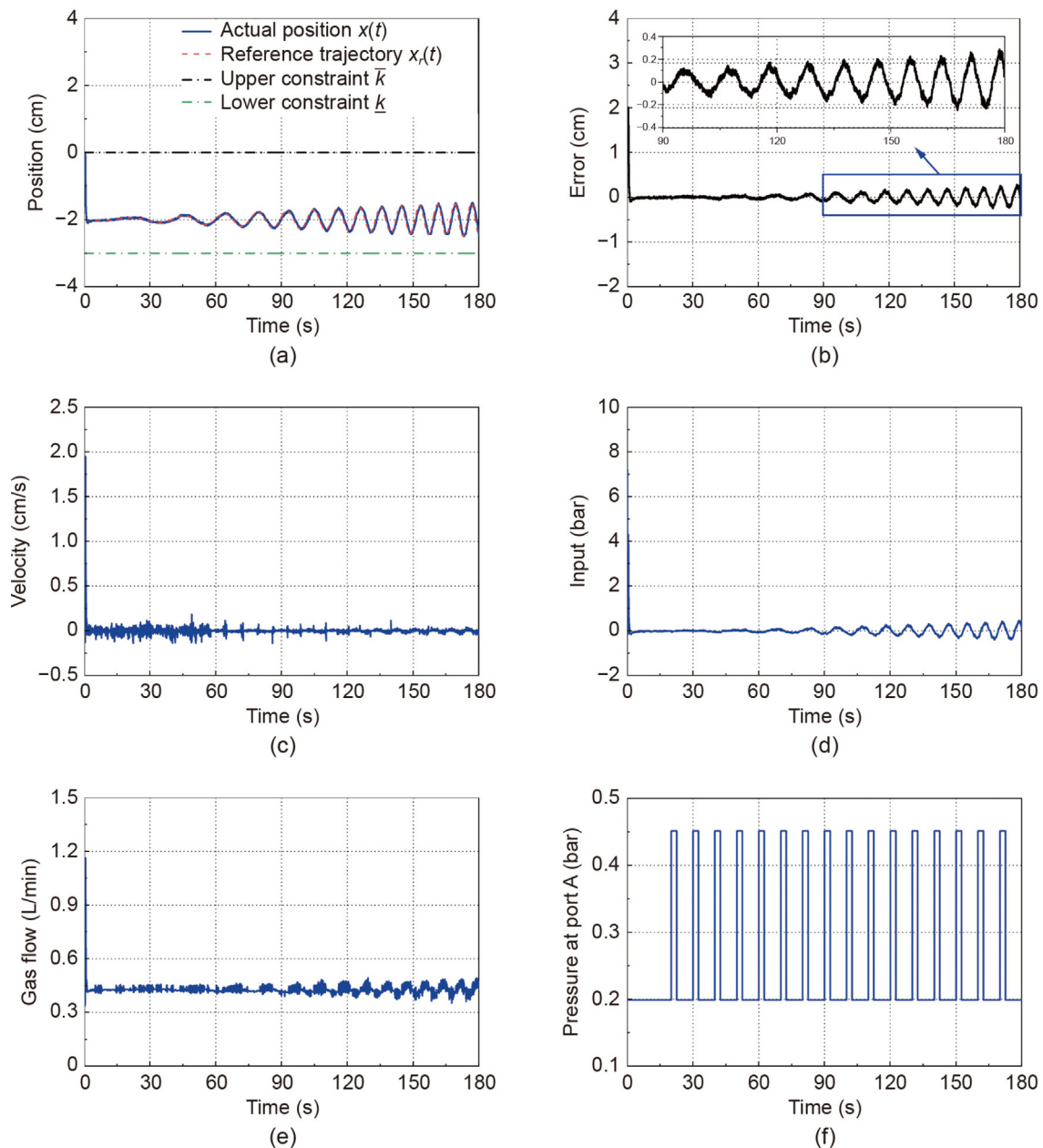


**Fig. 8.** Results employing the MFAC method. (a) Measured position and the reference position ( $x(t)$  and  $x_r(t)$ ). (b) Error between the measured position and the reference position ( $e(t)$  and  $w_1$ ). (c) Velocity of the PMA ( $\dot{x}(t)$  and  $w_2$ ). (d) Change of the control input ( $u(t)$ ). (e) Airflow of the PMA. (f) Air pressure at port A.

tracking of PMAs under unknown dynamics and output constraints. We characterized the stability analysis of the control method from a theoretical perspective. Further on, we validated the effectiveness of the presented control method by considering experimental results. This work we have presented is preliminary. While the current work is preliminary, future efforts will aim to extend this method to more complex robotic systems involving multiple PMAs.

#### CRediT authorship contribution statement

**Xingchen Li:** Writing – original draft, Validation, Writing – review & editing, Visualization, Data curation. **Xifeng Gao:** Methodology, Conceptualization, Supervision, Formal analysis.

#### Declaration of competing interest

The authors declare that they have no known competing financial interests or personal relationships that could have appeared to influence the work reported in this paper.

#### Acknowledgments

This work is supported by the National Natural Science Foundation of China (52305569), the China Postdoctoral Science Foundation, China (2023M740940), the Innovation Team Project for Ordinary Universities in Guangdong Province (2024KCXTD041), and program for scientific research start-upfunds of Guangdong Ocean University (060302062404).

## References

- [1] Y. Kim, Y. Lee, S. Lee, J. Kim, H.S. Kim, T. Seo, STEP: A new mobile platform with 2-DOF transformable wheels for service robots, *IEEE/ASME Trans. Mechatron.* 25 (4) (2020) 1859–1868, <http://dx.doi.org/10.1109/TMECH.2020.2992280>.
- [2] Y. Huang, E. Burdet, L. Cao, P.T. Phan, A.M.H. Tiong, S.J. Phee, A subject-specific four-degree-of-freedom foot interface to control a surgical robot, *IEEE/ASME Trans. Mechatron.* 25 (2) (2020) 951–963, <http://dx.doi.org/10.1109/TMECH.2020.2964295>.
- [3] M.F. Rox, D.S. Ropella, R.J. Hendrick, E. Blum, R.P. Naftel, H.C. Bow, S.D. Hurrell, K.D. Weaver, L.B. Chambless, R.J. Webster III, Mechatronic design of a two-arm concentric tube robot system for rigid neuroendoscopy, *IEEE/ASME Trans. Mechatron.* 25 (3) (2020) 1432–1443, <http://dx.doi.org/10.1109/TMECH.2020.2976897>.
- [4] H. Hassan, C. Dominguez, J. Martínez, A. Perles, J. Capella, J. Albaladejo, A multidisciplinary PBL robot control project in automation and electronic engineering, *IEEE Trans. Educ.* 58 (3) (2015) 167–172, <http://dx.doi.org/10.1109/TE.2014.2348538>.
- [5] T. Takeda, Y. Hirata, K. Kosuge, Dance step estimation method based on HMM for dance partner robot, *IEEE Trans. Ind. Electron.* 54 (2) (2007) 699–706, <http://dx.doi.org/10.1109/TIE.2007.891642>.
- [6] X. Gao, Y. Sun, L. Hao, H. Yang, Y. Chen, C. Xiang, A new soft pneumatic elbow pad for joint assistance with application to smart campus, *IEEE Access* 6 (2018) 38967–38976, <http://dx.doi.org/10.1109/ACCESS.2018.2852757>.
- [7] X. Gao, X. Li, J. Xiao, L. Hao, Robust PI-type output feedback control of unknown nonlinear systems, *IEEE Trans. Ind. Electron.* 69 (9) (2021) 9396–9405, <http://dx.doi.org/10.1109/TIE.2021.3112995>.
- [8] X. Gao, X. Li, Y. Sun, L. Hao, H. Yang, C. Xiang, Model-free tracking control of continuum manipulators with global stability and assigned accuracy, *IEEE Trans. Syst. Man, Cybern. Syst.* 69 (9) (2021) 9396–9405, <http://dx.doi.org/10.1109/TSMC.2020.30187565>.
- [9] X. Gao, J.-X. Zhang, L. Hao, Fault-tolerant control of pneumatic continuum manipulators under actuator faults, *IEEE Trans. Ind. Inform.* 17 (12) (2021) 8299–8307, <http://dx.doi.org/10.1109/TII.2021.3064576>.
- [10] X. Gao, X. Li, C. Zhao, L. Hao, C. Xiang, Variable stiffness structural design of a dual-segment continuum manipulator with independent stiffness and angular position, *Robot. Comput.-Integr. Manuf.* 67 (5) (2021) 102000, <http://dx.doi.org/10.1016/j.rcim.2020.102000>.
- [11] J. Zhang, J. Sheng, C.T. O'Neill, C.J. Walsh, R.J. Wood, J. Ryu, J.P. Desai, M.C. Yip, Robotic artificial muscles: Current progress and future perspectives, *IEEE Trans. Robot.* 35 (3) (2019) 761–781, <http://dx.doi.org/10.1109/TRO.2019.2894371>.
- [12] J. Burgner-Kahrs, D.C. Rucker, H. Choset, Continuum robots for medical applications: A survey, *IEEE Trans. Robot.* 31 (6) (2015) 1261–1280, <http://dx.doi.org/10.1109/TRO.2015.2489500>.
- [13] C.-P. Chou, B. Hannaford, Measurement and modeling of McKibben pneumatic artificial muscles, *IEEE Trans. Robot. Autom.* 12 (1) (1996) 90–102, <http://dx.doi.org/10.1109/70.481753>.
- [14] D.B. Reynolds, D.W. Repperger, C.A. Phillips, G. Bandry, Modeling the dynamic characteristics of pneumatic muscle, *Ann. Biomed. Eng.* 31 (3) (2003) 310–317, <http://dx.doi.org/10.1114/1.1554921>.
- [15] D. Zhang, X. Zhao, J. Han, Active model-based control for pneumatic artificial muscle, *IEEE Trans. Ind. Electron.* 64 (2) (2017) 1686–1695, <http://dx.doi.org/10.1109/TIE.2016.2606080>.
- [16] G. Andrikopoulos, G. Nikolakopoulos, I. Arvanitakis, S. Manesis, Piecewise affine modeling and constrained optimal control for a pneumatic artificial muscle, *IEEE Trans. Ind. Electron.* 61 (2) (2014) 904–916, <http://dx.doi.org/10.1109/TIE.2013.2254094>.
- [17] J. Wu, J. Huang, Y. Wang, K. Xing, Nonlinear disturbance observer-based dynamic surface control for trajectory tracking of pneumatic muscle system, *IEEE Trans. Control Syst. Technol.* 22 (2) (2014) 440–455, <http://dx.doi.org/10.1109/TCST.2013.2262074>.
- [18] H. Aschemann, D. Schindele, Sliding-mode control of a high-speed linear axis driven by pneumatic muscle actuators, *IEEE Trans. Ind. Electron.* 55 (11) (2008) 3855–3864, <http://dx.doi.org/10.1109/TIE.2008.2003202>.
- [19] C.P. Vo, X.D. To, K.K. Ahn, A novel adaptive gain integral terminal sliding mode control scheme of a pneumatic artificial muscle system with time-delay estimation, *IEEE Access* 7 (2019) 141133–141143, <http://dx.doi.org/10.1109/ACCESS.2019.2944197>.
- [20] Y. Qin, H. Zhang, X. Wang, J. Han, Active model-based hysteresis compensation and tracking control of pneumatic artificial muscle, *Sensors* 22 (1) (2022) 364, <http://dx.doi.org/10.3390/s22010364>.
- [21] G. Liu, N. Sun, T. Yang, Z. Liu, Y. Fang, Equivalent-input-disturbance rejection-based adaptive motion control for pneumatic artificial muscle arms via hysteresis compensation models, *Control. Eng. Pr.* 138 (2023) 105609, <http://dx.doi.org/10.1016/j.conengprac.2023.105609>.
- [22] K. Qian, Z. Li, S. Chakrabarty, Z. Zhang, S.Q. Xie, Robust iterative learning control for pneumatic muscle with uncertainties and state constraints, *IEEE Trans. Ind. Electron.* 70 (2) (2022) 1802–1810, <http://dx.doi.org/10.1109/TIE.2022.3159970>.
- [23] H. Zhang, Y. Li, Y. Guo, X. Chen, Q. Ren, Control of pneumatic artificial muscles with SNN-based cerebellar-like model, in: *International Conference on Social Robotics*, Springer, 2021, pp. 824–828, [http://dx.doi.org/10.1007/978-3-030-90525-5\\_79](http://dx.doi.org/10.1007/978-3-030-90525-5_79).
- [24] G. Andrikopoulos, G. Nikolakopoulos, S. Manesis, Development and control of a hybrid controlled vertical climbing robot based on pneumatic muscle actuators, *J. Control. Eng. Technol.* 1 (2) (2011) 53–58, <http://dx.doi.org/10.1007/s11771-009-0160-x>.
- [25] B. Tondur, Single linear integral action control for closed-loop positioning of a biomimetic actuator with artificial muscles, in: *Proc. Eur. Control Conf.*, 2015, pp. 3585–3590, <http://dx.doi.org/10.1109/ECC.2015.7331088>.
- [26] S.W. Chan, J.H. Lilly, D.W. Repperger, J.E. Berlin, Fuzzy PD+I learning control for a pneumatic muscle, in: *Proc. 12th IEEE Int. Conf. FUZZ.*, 2003, pp. 278–283, <http://dx.doi.org/10.1109/FUZZ.2003.1209375>.
- [27] K. Xing, Y. Wang, Q. Zhu, H. Zhou, Modeling and control of mckibben artificial muscle enhanced with echo state networks, *Control. Eng. Pr.* 20 (5) (2012) 477–488, <http://dx.doi.org/10.1016/j.conengprac.2012.01.002>.
- [28] D.X. Ba, T.Q. Dinh, K.K. Ahn, An integrated intelligent nonlinear control method for a pneumatic artificial muscle, *IEEE/ASME Trans. Mechatron.* 21 (4) (2016) 1835–1845, <http://dx.doi.org/10.1109/TMECH.2016.2558292>.
- [29] P. Carbonell, Z.P. Jiang, D.W. Repperger, A fuzzy backstepping controller for a pneumatic muscle actuator system, in: *Proc. IEEE Int. Symp. Intell. Control*, 2001, pp. 353–358, <http://dx.doi.org/10.1109/ISIC.2001.971535>.
- [30] H.I. Chen, M.C. Shih, Visual control of an automatic manipulation system by microscope and pneumatic actuator, *IEEE Trans. Autom. Sci. Eng.* 10 (1) (2013) 215–218, <http://dx.doi.org/10.1109/TASE.2012.2205239>.
- [31] Y. Song, Y. Wang, C. Wen, Adaptive fault-tolerant PI tracking control with guaranteed transient and steady-state performance, *IEEE Trans. Autom. Control* 62 (1) (2017) 481–487, <http://dx.doi.org/10.1109/TAC.2016.2554362>.
- [32] N. Sun, D. Liang, Y. Wu, Y. Chen, Y. Qin, Y. Fang, Adaptive control for pneumatic artificial muscle systems with parametric uncertainties and unidirectional input constraints, *IEEE Trans. Ind. Inf.* 16 (2) (2020) 969–979, <http://dx.doi.org/10.1109/TII.2019.2923715>.
- [33] Q. Ai, D. Ke, J. Zuo, W. Meng, Q. Liu, Z. Zhang, S.Q. Xie, High-order model-free adaptive iterative learning control of pneumatic artificial muscle with enhanced convergence, *IEEE Trans. Ind. Electron.* 67 (11) (2020) 9548–9559, <http://dx.doi.org/10.1109/TIE.2019.2952810>.
- [34] J.-P. Cai, F. Qian, R. Yu, L. Shen, Adaptive control for a pneumatic muscle joint system with saturation input, *IEEE Access* 8 (2020) 117698–117705, <http://dx.doi.org/10.1109/ACCESS.2020.3004823>.
- [35] L. Zhu, X. Shi, Z. Chen, H. Zhang, C. Xiong, Adaptive servomechanism of pneumatic muscle actuators with uncertainties, *IEEE Trans. Ind. Electron.* 64 (4) (2017) 3329–3337, <http://dx.doi.org/10.1109/TIE.2016.2573266>.
- [36] H. Li, D. Gong, J. Yu, Control of robotic joint actuated by antagonistic pneumatic artificial muscles based on model-free reinforcement learning, in: *2021 IEEE International Conference on Robotics and Biomimetics, ROBIO*, IEEE, 2021, pp. 887–892, <http://dx.doi.org/10.1109/ROBIO54168.2021.9739393>.
- [37] G. Liu, N. Sun, T. Yang, Y. Fang, Reinforcement learning-based prescribed performance motion control of pneumatic muscle actuated robotic arms with measurement noises, *IEEE Trans. Syst. Man Cybern. Syst.* 53 (3) (2022) 1801–1812, <http://dx.doi.org/10.1109/TSMC.2022.3207575>.
- [38] Y. Li, Q. Liu, W. Meng, Y. Xie, Q. Ai, S.Q. Xie, MISO model free adaptive control of single joint rehabilitation robot driven by pneumatic artificial muscles, in: *2020 IEEE/ASME International Conference on Advanced Intelligent Mechatronics, AIM*, IEEE, 2020, pp. 1700–1705, <http://dx.doi.org/10.1109/AIM43001.2020.9158805>.
- [39] Z. Zhao, L. Hao, M. Liu, H. Gao, X. Li, Prescribed performance model-free adaptive terminal sliding mode control for the pneumatic artificial muscles elbow exoskeleton, *J. Mech. Sci. Technol.* 35 (2021) 3183–3197, <http://dx.doi.org/10.1007/s12206-021-0639-4>.
- [40] J. Zhang, G. Yang, Prescribed performance fault-tolerant control of uncertain nonlinear systems with unknown control directions, *IEEE Trans. Autom. Control* 62 (12) (2017) 6529–6535, <http://dx.doi.org/10.1109/TAC.2017.2705033>.
- [41] J. Zhang, G. Yang, Fuzzy adaptive output feedback control of uncertain nonlinear systems with prescribed performance, *IEEE Trans. Cybern.* 48 (5) (2018) 1342–1354, <http://dx.doi.org/10.1109/TCYB.2017.2692767>.
- [42] S. He, S. Dai, F. Luo, Asymptotic trajectory tracking control with guaranteed transient behavior for MSV with uncertain dynamics and external disturbances, *IEEE Trans. Ind. Electron.* 66 (5) (2019) 3712–3720, <http://dx.doi.org/10.1109/TIE.2018.2842720>.
- [43] J.-X. Zhang, G.-H. Yang, Adaptive prescribed performance control of nonlinear output-feedback systems with unknown control direction, *Internat. J. Robust Nonlinear Control* 28 (16) (2018) 4696–4712, <http://dx.doi.org/10.1002/rnc.4277>.

- [44] X. Jin, Adaptive fault-tolerant control for a class of output-constrained nonlinear systems, *Internat. J. Robust Nonlinear Control* 59 (2015) 200–205, <http://dx.doi.org/10.1002/rnc.3293>.
- [45] J.-X. Zhang, G.-H. Yang, Robust adaptive fault-tolerant control for a class of unknown nonlinear systems, *IEEE Trans. Ind. Electron.* 64 (1) (2017) 585–594, <http://dx.doi.org/10.1109/TIE.2016.2595481>.
- [46] S. El-Ferik, H.A. Hashim, F.L. Lewis, Neuro-adaptive distributed control with prescribed performance for the synchronization of unknown nonlinear networked systems, *IEEE Trans. Syst. Man, Cybern. Syst.* 48 (12) (2018) 2135–2144, <http://dx.doi.org/10.1109/TSMC.2017.2702705>.
- [47] H. Yang, Q.-L. Han, X. Ge, L. Ding, Y. Xu, B. Jiang, D. Zhou, Fault-tolerant cooperative control of multiagent systems: A survey of trends and methodologies, *IEEE Trans. Ind. Inf.* 16 (1) (2020) 4–17, <http://dx.doi.org/10.1109/TII.2019.2945004>.
- [48] J.-X. Zhang, G.-H. Yang, Fault-tolerant fixed-time trajectory tracking control of autonomous surface vessels with specified accuracy, *IEEE Trans. Ind. Electron.* 67 (6) (2020) 4889–4899, <http://dx.doi.org/10.1109/TIE.2019.2931242>.
- [49] Z. Hou, S. Jin, Data-driven model-free adaptive control for a class of MIMO nonlinear discrete-time systems, *IEEE Trans. Neural Netw.* 22 (12) (2011) 2173–2188, <http://dx.doi.org/10.1109/TNN.2011.2176141>.